Plant Physiology and Biochemistry 136 (2019) 43–51

Contents lists available at ScienceDirect

Plant Physiology and Biochemistry

journal homepage: www.elsevier.com/locate/plaphy

Research article

# Exogenous application of cytokinin during dark senescence eliminates the acceleration of photosystem II impairment caused by chlorophyll *b* deficiency in barley

Helena Janečková, Alexandra Husičková, Dušan Lazár, Ursula Ferretti, Pavel Pospíšil, Martina Špundová*

*Centre of the Region Haná for Biotechnological and Agricultural Research, Department of Biophysics, Faculty of Science, Palacký University, Šlechtitelů 241/27, Olomouc, 783 71, Czech Republic*

ARTICLE INFO

*Keywords:*
6-Benzylaminopurine
Chlorina
Chlorophyll fluorescence
Leaf senescence
OJIP
Photosystem II photochemistry
Xanthophylls

ABSTRACT

Recent studies have shown that chlorophyll (Chl) *b* has an important role in the regulation of leaf senescence. However, there is only limited information about senescence of plants lacking Chl *b* and senescence-induced decrease in photosystem II (PSII) and photosystem I (PSI) function has not even been investigated in such plants. We have studied senescence-induced changes in photosynthetic pigment content and PSII and PSI activities in detached leaves of Chl *b*-deficient barley mutant, *chlorina f2*$^{f2}$ (*clo*). After 4 days in the dark, the senescence-induced decrease in PSI activity was smaller in *clo* compared to WT leaves. On the contrary, the senescence-induced impairment in PSII function (estimated from Chl fluorescence parameters) was much more pronounced in *clo* leaves, even though the relative decrease in Chl content was similar to wild type (WT) leaves (*Hordeum vulgare* L., cv. Bonus). The stronger impairment of PSII function seems to be related to more pronounced damage of reaction centers of PSII. Interestingly, exogenously applied plant hormone cytokinin 6-benzylaminopurine (BA) was able to maintain PSII function in the dark senescing *clo* leaves to a similar extent as in WT. Thus, considering the fact that without BA the senescence-induced decrease in PSII photochemistry in *clo* was more pronounced than in WT, the relative protective effect of BA was higher in Chl *b*-deficient mutant than in WT.

## 1. Introduction

Leaf senescence, a final stage of leaf life preceding its death, is important for plant with respect to nutrient remobilization. Leaf senescence is accompanied by a massive degradation of chlorophyll (Chl) and by inhibition of photosynthetic processes including photosystem II (PSII) photochemistry (Oh et al., 1996; Špundová et al., 2003, 2005; Vlčková et al., 2006; Kusaba et al., 2007; Talla et al., 2016; Janečková et al., 2018) and photosystem I (PSI) activity (Nath et al., 2013; Krieger-Liszkay et al., 2015). In the literature, there is no consensus whether the decrease of photosynthetic activity of PSII precedes the inhibition of PSI or *vice versa* (e.g., Nath et al., 2013; Krieger-Liszkay et al., 2015).

Leaf senescence is regulated by many factors, including plant hormones cytokinins. Cytokinins are known to slow down senescence, decelerate senescence-associated degradation of photosynthetic pigments and deterioration of photosynthetic function (Oh et al., 2005; Vlčková et al., 2006; Talla et al., 2016; Vylíčilová et al., 2016). Recent investigations have shown that Chl *b* also plays an important role in the regulation of leaf senescence. Mutants with higher Chl *b* content appear to have slower senescence-related degradation of Chl, light-harvesting

*Abbreviations: ABS/RC*, apparent antenna size of active reaction center of photosystem II; BA, 6-benzylaminopurine; CAO, chlorophyllide *a* oxygenase; car, carotenoids (sum of carotenes and xanthophylls); Chl, chlorophyll; *clo*, *chlorina f2*$^{f2}$ mutant; DEPS, the de-epoxidation state of xanthophylls; $(dV/dt)_0$, the initial slope of the O-J chlorophyll fluorescence rise; $F_v/F_m$, maximal quantum yield of photosystem II photochemistry in the dark-adapted state; $F_v'/F_m'$, the maximal quantum yield of photosystem II photochemistry in the light-adapted state; LHC(s), light-harvesting complex(es); OJIP, chlorophyll fluorescence induction transient; PSI, photosystem I; PSII, photosystem II; P700, primary electron donor of photosystem I; RCI, reaction center(s) of photosystem I; RCII, reaction center(s) of photosystem II; $RE_0/ABS$, quantum yield of electron transport from reduced $Q_A$ to final acceptors of photosystem I; VAZ, content of xanthophylls (violaxanthin, antheraxanthin, and zeaxanthin); $V_J$, the relative variable fluorescence at the J step of OJIP curve; $\delta R_0$, the efficiency of electron transport from reduced plastoquinone to final acceptors of photosystem I; $\Phi_{f,D}$, quantum yield of constitutive non-regulatory dissipation processes in the light-adapted state; $\Phi_{NPQ}$, quantum yield of regulatory non-photochemical quenching in the light-adapted state; $\Phi_P$, the effective quantum yield of PSII photochemistry in the light-adapted state

* Corresponding author.
*E-mail address:* martina.spundova@upol.cz (M. Špundová).

https://doi.org/10.1016/j.plaphy.2019.01.005
Received 21 September 2018; Received in revised form 19 December 2018; Accepted 3 January 2019
Available online 04 January 2019
0981-9428/ 

complexes (LHCs) and thylakoid membranes (Kusaba et al., 2007; Sakuraba et al., 2012; Voitsekhovskaja and Tyutereva, 2015). At the same time, a recent study with *pgl* rice mutant has shown that Chl *b* deficiency was associated with increased Chl degradation, accumulation of reactive oxygen species, and electrolyte leakage during both natural senescence of flag leaves and dark-induced senescence of detached leaves (Yang et al., 2016). Kusaba et al. (2007) has also mentioned faster Chl degradation in dark-incubated detached leaves of *cao-2* rice mutant deficient in Chl *b*. Although these studies suggest that senescence-related changes are accelerated in plants lacking Chl *b*, the question whether and how Chl *b* deficiency affects senescence-induced inhibition of PSII and PSI function has not been addressed yet.

In order to broaden knowledge about the effect of missing Chl *b* on senescence, we have studied the changes in Chl and carotenoid (car) content and changes in PSII and PSI activity in dark-senescing detached leaves of *chlorina f2*$^{f2}$ (*clo*) barley mutant. The *clo* mutant is deficient in Chl *b* due to the mutation in chlorophyllide *a* oxygenase (CAO), the enzyme responsible for the conversion of chlorophyllide *a* to chlorophyllide *b* and thus crucial for biosynthesis of Chl *b* (Mueller et al., 2012). The *clo* mutant has also lower contents of Chl *a* and car compared to WT (Štroch et al., 2004, 2008). The mutant is deficient in light-harvesting complexes Lhcb1, Lhcb6 and Lhca4, and has reduced amount of Lhcb2, Lhcb3 and Lhcb4 (Bossmann et al., 1997). The amount of LHCs of PSII and PSI is reduced by about 80 % and 20 %, respectively (Ghirardi et al., 1986). The more reduced amount of LHCs of PSII (LHCII) is in *chlorina* mutants compensated by an increased amount of reaction centers of PSII (RCII) and a greater ratio of RCII/RCI (Ghirardi et al., 1986).

The *chlorina* mutants generally have similar or only slightly lower efficiency of PSII photochemistry (Leverenz et al., 1992; Štroch et al., 2004, 2008) and oxygen evolution (Havaux and Tardy, 1997) than WT plants. However, under stress conditions such as high light or high temperature, the PSII efficiency is more reduced in the mutants (Leverenz et al., 1992; Havaux and Tardy, 1997; Peng et al., 2002; Štroch et al., 2008; Tyutereva et al., 2017) than in WT. The increased stress-sensitivity of the PSII photochemistry in the *chlorina* mutant has been attributed to its reduced amount of LHCs, resulting from missing Chl *b* (Havaux and Tardy, 1997).

In this work, we have studied how the Chl *b* deficiency in *clo* mutant changes the progress of dark senescence of detached leaves, with special focus given on the description of senescence-induced changes in the function of PSII. As cytokinins are known decelerators of senescence, we also wanted to find out whether and to what extent is exogenously applied cytokinin 6-benzylaminopurine able to suppress the supposedly pronounced senescence in Chl *b*-deficient *clo* mutant.

## 2. Materials and methods

### 2.1. Plant material and growth conditions

Seeds of wild-type barley (*Hordeum vulgare* L. cv. Bonus; WT) and *chlorina f2*$^{f2}$ (*clo*) mutant were soaked in deionized water for 24 h before sowing and then transferred into pots containing perlite with Hoagland solution. Pots were placed in a growth chamber under controlled conditions of 16 h light (150 µmol of photons $m^{-2}$ $s^{-1}$)/8 h dark, 22/20 °C and 60% relative air humidity.

Eight days after the sowing, 4-cm segments were cut off from the primary leaves. Leaf segments were placed either into a 0.2% solution of dimethylsulfoxide (DMSO) or into a $10^{-5}$ mol $l^{-1}$ solution of 6-benzylaminopurine (BA) in 0.2% DMSO (BA treated leaves). The leaf segments were then kept in the dark (other conditions were same as during plant growth). Measurements were performed immediately after the leaf detachment and on the 4th day after detachment.

### 2.2. Pigment analysis

For the determination of the content of pigments, the area of leaf samples was estimated and then the leaves were homogenized in liquid nitrogen, with $MgCO_3$ and 80% acetone. The homogenates were centrifuged at 4,000*g* and 4 °C for 10 min. The supernatant was used for the spectrophotometric estimation of Chl and total car contents (a sum of carotenes and xanthophylls) according to Lichtenthaler (1987) by a spectrophotometer Unicam UV550 (ThermoSpectronic, United Kingdom) and also for the quantification of individual xanthophylls (violaxanthin, V; antheraxanthin, A; zeaxanthin, Z) by high performance liquid chromatography (HPLC).

For the estimation of xanthophyll content (VAZ) by an HPLC system (Alliance e 2695 HPLC System, Waters, USA), the supernatant was filtered through 0.45µm PTFE membrane (Acrodisc, Waters, USA) into dark vials. The amount of 100 µl was injected into the HPLC system. A LiChroCART RP-18 (5 µm; 4.6 × 250 mm) column (Merck & Co., USA) was used. The analysis was performed by a gradient reverse-phase analysis (1.5 ml $min^{-1}$ at 25 °C). The analysis started with isocratic elution using the mobile phase composed of acetonitrile, methanol and 0.1 mol $l^{-1}$ Tris (pH 8) in the ratio 87:10:3 (v:v:v) for 10 min and was followed by a 2-min linear gradient using mobile phase composed of a mixture of methanol and n-hexane in the ratio 4:1 (v:v). Absorbance was detected at 440 nm using UV/VIS detector. The amount of pigments in samples was determined using their conversion factors (Färber and Jahns, 1998). The de-epoxidation state of xanthophylls (DEPS) was calculated according to Gilmore and Björkman (1994) as $(A + Z)/(V + A + Z) \times 100$ (%).

### 2.3. Chlorophyll fluorescence measurements

The Chl fluorescence induction transient (OJIP curves) and the quenching analysis were measured at room temperature on adaxial side of leaf samples. Freshly detached leaves (i.e., leaves before senescence induction) were dark-adapted for 25 min before the measurement. The OJIP curves were measured in the middle of leaf segments by Plant Efficiency Analyser (Hansatech Instruments, United Kingdom) for 2 s with excitation light intensity of 1100 µmol of photons $m^{-2}$ $s^{-1}$. The initial slope of the O-J Chl fluorescence rise $(dV/dt)_O$, the relative variable fluorescence at the J step ($V_J$), and the specific energy flux *ABS/RC* were evaluated as follows (see Stirbet et al., 2018). The $(dV/dt)_O = 4(F_{300\mu s} - F_{50\mu s})/F_v$, where $F_{300\mu s}$ and $F_{50\mu s}$ are fluorescence intensities at the indicated times and $F_v$ is variable fluorescence ($F_v = F_p - F_O$; $F_0$ is a minimal fluorescence and $F_p$ is fluorescence at the P step). The $(dV/dt)_O$ parameter, defined as the maximal rate of the accumulation of the fraction of closed reaction centers of PSII (RCII) (Strasser et al., 2000), reflects the rate of excitation supply into the RCII and subsequently the rate of $Q_A$ reduction. Parameter $V_J$, reflecting the fraction of reduced $Q_A$, was calculated as $(F_J - F_0)/F_v$, where $F_J$ is fluorescence intensity at 2 ms. *ABS/RC* was calculated as $(dV/dt)_O/V_J \times F_p/F_v$ and reflects apparent antenna size of active RCII (Strasser et al., 2000). Further, the quantum yield of electron transport from reduced $Q_A$ to final acceptors of PSI ($RE_O/ABS$) and the efficiency of electron transport from reduced plastoquinone to final acceptors of PSI ($\delta R_0$) were estimated as follows: $RE_O/ABS = F_v/F_p \times (1 - V_I)$ and $\delta R_O = (1 - V_I)/(1 - V_J)$ (Stirbet et al., 2018). The measured OJIP curves as well as curves normalized to $F_v$ are presented.

The quenching analysis was performed using PlantScreen (Photon Systems Instruments, Czech Republic) phenotyping platform (Humplík et al., 2015) according to the following protocol. At the beginning, the minimal fluorescence $F_0$ was determined using measuring flashes (duration of 10 µs) of red light (650 nm), which did not cause any closure of RCII. Then a saturating pulse (white light, 1900 µmol of photons $m^{-2}$ $s^{-1}$, duration of 800 ms) was applied to measure maximal fluorescence $F_m$. After 90 s of dark-relaxation, when the measured fluorescence signal reached $F_0$, the leaf samples were exposed to actinic

light for 25 min (red light, 150 μmol of photons $m^{-2}$ $s^{-1}$, the same intensity as used for plant growth). To determine the maximal fluorescence during the actinic light exposition ($F_m'$), a set of the saturating pulses was applied. The first pulse was applied 10 s after the actinic light was switched on and was followed by 9 pulses in 20 s intervals and then by 22 pulses in 59 s intervals.

The maximal quantum yield of PSII photochemistry in the dark-adapted state was estimated as $F_v/F_m = (F_m - F_0)/F_m$. The maximal quantum yield of PSII photochemistry in the light-adapted state was calculated as $F_v'/F_m' = (F_m' - F_0')/F_m'$, where $F_0'$ is minimal fluorescence for the light-adapted state, which was calculated as $F_0/(F_v/F_m + F_0/F_m')$. The effective quantum yield of PSII photochemistry in the light-adapted state was calculated as $\Phi_P = (F_m' - F_t)/F_m'$, where $F_t$ is fluorescence at time t measured immediately prior to the application of the saturating pulse. The quantum yield for regulatory non-photochemical quenching was calculated as $\Phi_{NPQ} = (F_t/F_m') - (F_t/F_m)$ and the quantum yield for constitutive non-regulatory dissipation processes was calculated as $\Phi_{f,D} = F_t/F_m$. The sum of $\Phi_P$, $\Phi_{NPQ}$ and $\Phi_{f,D}$ equals unity (for a review, see Lazár, 2015). In the case of $F_v'/F_m'$, $\Phi_P$, $\Phi_{NPQ}$, and $\Phi_{f,D}$, values obtained at the end of the actinic light exposition are presented.

### 2.4. Measurement of P700 oxidation

For estimation of light-induced oxidation of P700 (the primary electron donor of PSI), the I830 signal as a difference of transmittance at 875 nm and 830 nm was determined using Dual PAM 100 (Walz, Germany), see, e.g. Lazár (2013). The methodology assumes that P700 is fully reduced in the dark-adapted leaf and thus the I830 signal is zero. During illumination of the leaf, the I830 signal rises to a peak level reflecting an equilibrated maximal $P700^+$ level as a result of P700 oxidation by the charge separation and $P700^+$ reduction by plastocyanin. In both WT and *clo* leaves before senescence induction, the I830 signal reached the peak level at 17 ms. In senescing leaves, the level of $P700^+$ at 17 ms of illumination was expressed in % of the peak level observed in the leaves before senescence induction.

### 2.5. Statistical analysis

In all statistical testing, related data sets were first tested for normality (Kolmogorov-Smirnov test with Lilliefors' correction) and equality of variances (Levene Median test). If fulfilled, the Student's *t*-test or ANOVA test (with all pairwise multiple comparison by Holm-Sidak *post hoc* test) were used and if not fulfilled, the Mann-Whitney Rank Sum test or Kruskal-Wallis ANOVA on Ranks test (with all pairwise multiple comparison by Dunn's *post hoc* test) were used. The critical level of 0.05 was chosen for all tests (the P-value of the test is marked by *). If the P-value of a test was even lower than 0.01 or even lower than 0.001, the results are marked by ** or ***, respectively. All testing was performed using SigmaPlot version 11 (Systat Software, USA).

## 3. Results

### 3.1. Characterization of clo leaves before senescence induction

Leaves of the *clo* mutant had approximately half the Chl content compared to WT (Table 1). The content of Chl *a* was lower by about 30 %, while Chl *b* was not detected (Table 1). The content of carotenoids (car; sum of carotenes and xanthophylls) was also lower in *clo* (by about 30 % compared to WT). As a result of relatively more lowered content of Chl than car, *clo* had significantly lower *Chl/car* ratio than the WT (Table 1). Leaves of *clo* had also lower content of xanthophylls (VAZ) (by about 25 %; Table 1). However, the *VAZ/Chl* ratio and de-epoxidation state of the xanthophyll cycle pigment pool (DEPS) were higher in *clo* (Table 1), which indicates better photoprotection of photosynthetic apparatus in *clo* compared to WT.

**Table 1**
The content of pigments (mg per $m^2$ of leaf area), their ratios and maximal efficiency of PSII photochemistry in dark- ($F_v/F_m$) and light-adapted ($F_v'/F_m'$) state in leaves of WT and *clo* mutant before senescence induction.

| | WT | *clo* |
|---|---|---|
| Chl *a* | 176 ± 24 | **121 ± 4** |
| Chl *b* | 51 ± 7 | n. d. |
| Chl *a*+*b* | 227 ± 31 | **121 ± 4** |
| Chl *a*/*b* | 3.4 ± 0.1 | n. d. |
| car | 43 ± 5 | **30 ± 1** |
| *Chl/car* | 5.3 ± 0.4 | **4.0 ± 0.1** |
| VAZ | 16.6 ± 1.5 | **12.3 ± 1.0** |
| *VAZ/Chl* | 0.074 ± 0.004 | **0.102 ± 0.006** |
| DEPS (%) | 2.4 ± 1.0 | **4.3 ± 0.6** |
| $F_v/F_m$ | 0.802 ± 0.011 | **0.792 ± 0.004** |
| $F_v'/F_m'$ | 0.776 ± 0.003 | **0.720 ± 0.010** |

Means and SD (n = 3–10 for pigments and n = 6 for fluorescence parameters) are presented; n. d., not determined. Statistically significant differences (compared to WT, $P < 0.05$, *t*-test, except of DEPS where Mann-Whitney Rank Sum test was used) are indicated in bold.

Besides the generally reduced content of photosynthetic pigments, the maximal quantum yield of PSII photochemistry in both dark-adapted state ($F_v/F_m$) and light-adapted state ($F_v'/F_m'$) was slightly lowered in *clo* (Table 1, Fig. 1C). To determine whether *clo* had altered partitioning of absorbed light energy for photochemical and non-photochemical processes, the following parameters were evaluated in the light-adapted state: the effective quantum yield of PSII photochemistry ($\Phi_P$), quantum yield of constitutive non-regulatory dissipation processes ($\Phi_{f,D}$) and quantum yield of regulatory non-photochemical quenching ($\Phi_{NPQ}$). Together the sum of these quantum yields equals unity (Lazár, 2015). In *clo,* a slightly but significantly lower $\Phi_P$ and higher $\Phi_{f,D}$ and $\Phi_{NPQ}$ were observed (Fig. 1D), which indicates that lower fraction of absorbed light energy was used by PSII photochemistry and that more absorbed energy was dissipated *via* non-photochemical quenching processes.

As the *clo* mutant is deficient in Chl *b* (Table 1) and consequently in LHCII (Ghirardi et al., 1986; Bossmann et al., 1997), a lower supply of excitations from LHCII to RCII can be expected. It should affect transient of Chl fluorescence induction (OJIP curve), as this curve reflects closure of RCII (Lazár, 2006) that depends on the rate of excitation supply. The typical OJIP curve was observed in the *clo* leaves, although the overall fluorescence signal was lower compared to WT (Fig. 2A). From normalized curves it is obvious that the J- and I-steps are both reached later in the *clo* leaves (Fig. 2B) than in WT, which reflects a slower reduction of $Q_A$ as well as $Q_B$. This slower reduction consequently results in a lower transient accumulation of reduced $Q_A$, which is in turn reflected in a lower J-step. The lower relative height of J-step is quantitatively expressed by a lower $V_J$ parameter (by about 14 %) (Fig. 2B and C). The slower $Q_A$ reduction in the *clo* leaves is further indicated by $(dV/dt)_o$, which was lower by about 40 % (Fig. 2C) than in WT. Finally, a lower *ABS/RC* ratio (by about 25 % compared to WT; Fig. 2C) confirmed deficiency of LHCII in the *clo* leaves, as this ratio reflects an apparent antenna size of active RCII (Stirbet et al., 2018).

On the other hand, parameters of the OJIP curve reflecting electron transport to PSI, $RE_o/ABS$ (the quantum yield of electron transport from reduced $Q_A$ to final acceptors of PSI) and $\delta_{R0}$ (the efficiency of electron transport from reduced plastoquinone to final acceptors of PSI) were higher in *clo* by 46 and 44 %, respectively (Fig. 2D). Finally, a relative amount of $P700^+$ was lower in *clo* (Fig. 2D).

### 3.2. Comparison of dark senescence-induced changes in WT and clo detached leaves

To induce senescence, leaves of WT and *clo* were detached and

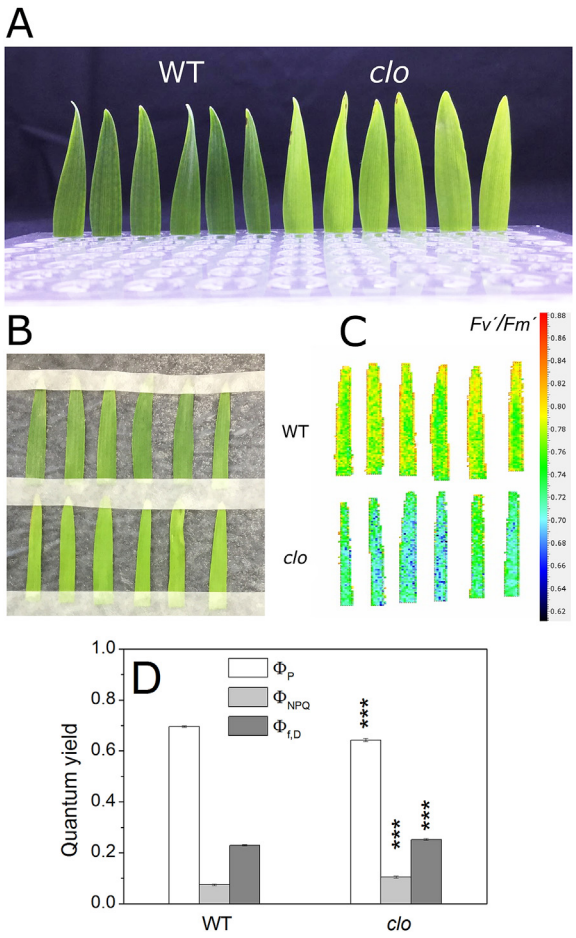


**Fig. 1.** Characterization of detached WT and *clo* leaves before senescence induction. A, phenotype; B, leaf segments used for the measurement of $F_v'/F_m'$; C, $F_v'/F_m'$ in the area of the leaf segments; D, quantum yield of PSII photochemistry ($\Phi_P$), regulatory non-photochemical quenching ($\Phi_{NPQ}$), and constitutive non-regulatory dissipation processes ($\Phi_{f,D}$). Means and SD are presented, n = 6–10. Asterisks indicate statistically significant difference (Student's *t*-test) between WT and *clo* ($P < 0.001$).

subsequently incubated in control solution (0.2% DMSO) in the dark for 4 days. This incubation resulted in a significant decrease in Chl, car and VAZ content in all detached leaves (Fig. 3). The Chl content decreased by 82 % in WT and 87 % in *clo* (Fig. 3) and although the relative decrease in Chl content was similar in WT and *clo*, the absolute Chl content was pronouncedly lower in the *clo* senescing leaves (about 16 mg Chl $m^{-2}$ compared to about 40 mg Chl $m^{-2}$ in WT). As indicated by a decrease in Chl *a/b* ratio, the content of Chl *a* decreased in WT slightly more than Chl *b* (Fig. 3).

The content of car decreased in WT by about 60 %, whereas in *clo* this content was reduced only by about 40 % (Fig. 3). Similarly, the VAZ content decreased more in WT (by about 70 %) than in *clo* (by about 55 %; Fig. 3). The faster breakdown of Chl compared to car caused a significant decrease in the *Chl/car* ratio in both genotypes, more pronounced in *clo* (Fig. 3). In summary, the relative decrease in Chl content was similar in both *clo* and WT, but the relative decrease in the content of car and VAZ in *clo* was lower than in WT.

The loss of photosynthetic pigments during dark-induced senescence was associated with a decline in the maximal quantum yield of PSII photochemistry in the dark-adapted state in both *clo* and WT. Parameter $F_v/F_m$ dropped by about 45 % in WT leaves and by about 70 % in *clo* (Fig. 4A), which indicates more pronounced impairment of PSII function in *clo* compared to WT. In fact, the real impairment of PSII function was much more pronounced in *clo*, because a considerable part of the area of measured leaves was already not photosynthetically functional enough for Chl fluorescence detection (i.e., the Chl fluorescence signal from *clo* leaves was so small that it was not distinguishable from a background signal, Fig. 4B) and these leaf parts were not included into the average $F_v/F_m$ value (Fig. 4A). Thus the average $F_v/F_m$ value is representative only for the (minimally) functional parts of leaves.

The decrease in $F_v/F_m$ was accompanied by a decrease in $\Phi_P$ in both *clo* and WT, indicating decreased energy utilization by PSII photochemistry in the light-adapted state. The $\Phi_P$ value in *clo* was significantly lower than in WT (Fig. 5). On the other hand, $\Phi_{NPQ}$ and $\Phi_{f,D}$ increased in senescing leaves, indicating enhanced energy dissipation by means of non-photochemical processes. Unlike the leaves before senescence induction, the partitioning of absorbed light energy into regulatory or non-regulatory dissipation processes differed pronouncedly in WT and *clo*. While $\Phi_{NPQ}$ and $\Phi_{f,D}$ were comparable in WT, in *clo* $\Phi_{f,D}$ prevailed (Fig. 5). It indicates that in WT, energy non-utilized by PSII photochemistry was dissipated in both regulatory and non-regulatory processes to a similar extent, while in *clo*, the majority of this energy was dissipated *via* non-regulatory processes. This corresponds to the extreme impairment of PSII function in *clo* (Fig. 4B).

After 4 days of incubation in the dark, the shape of OJIP curve and the height of its individual steps changed in WT as well as in *clo* (compare Figs. 2A and 6A). In senescing WT leaves, the OJIP curve was more flat than in non-senescing ones due to the pronounced increase in the height of the O-step and decrease in the height of the P-step (Fig. 6A). Additionally, the normalized curve showed a relative increase in the J-step (compare Figs. 2B and 6B), reflected also in the increased parameter $V_J$ (1.5-times when compared to leaves before senescence induction; Fig. 6C). The $(dV/dt)_o$ parameter also increased, but more (2.5-times) than $V_J$, thus *ABS/RC* proportional to their ratio increased more pronouncedly (4-times). The increase of *ABS/RC* suggests increase in apparent antenna size of active RCII, which in turn indicates preferential impairment of RCII compared to LHCII. This results in increased supply of excitations to remaining active RCII and thus a pronounced $Q_A$ reduction can be observed in these RCII. We propose that the preferential RCII impairment was caused by their degradation, as the Chl *a/b* ratio decreased in the WT senescing leaves (Fig. 3). Since Chl *b* occurs mainly in LHCII, the decrease in the Chl *a/b* ratio reflects a relative decrease in RCII abundance (Leong and Anderson, 1984).

$RE_o/ABS$ as well as $\delta R_0$ decreased in the senescing WT leaves by about 80 % and 45 %, respectively (Fig. 6D). The greater decrease in $RE_o/ABS$ in comparison to $\delta R_0$ indicates that the electron transport efficiency decreased more within PSII than behind PSII and that RCI degradation was lower than degradation of RCII. This assumption is supported by a lower relative amount of $P700^+$ (Fig. 6D).

In senescing leaves of *clo*, changes in the OJIP curve were much more profound than in WT. The typical OJIP shape was missing and the curve became almost flat (compare Figs. 2A and 6A). The relative height of the J-step increased ($V_J$ increased twice compared to the leaves before senescence), $(dV/dt)_o$ increased 4-times and *ABS/RC* increased 15-times (Fig. 6B and C). The extreme increase in *ABS/RC* was related also to very pronounced decrease in $F_v/F_m$. It means that the impairment of RCII during dark-senescence was much more pronounced in *clo* than in WT, which corresponds to more severe inhibition of PSII photochemistry described above.

Similarly to WT, parameters of the OJIP curve reflecting electron transport to PSI, $RE_o/ABS$ and $\delta R_0$, decreased in the senescing leaves of *clo* (Fig. 6D). The decrease was again more pronounced in the case of $RE_o/ABS$ (by 98 %) than in $\delta R_0$ parameter (by about 70 %), which indicates more pronounced impairment of electron transport within PSII than behind this complex and the preferential decrease in RCII compared to RCI. The relative amount of $P700^+$ was higher than in the senescing leaves of WT (Fig. 6D).

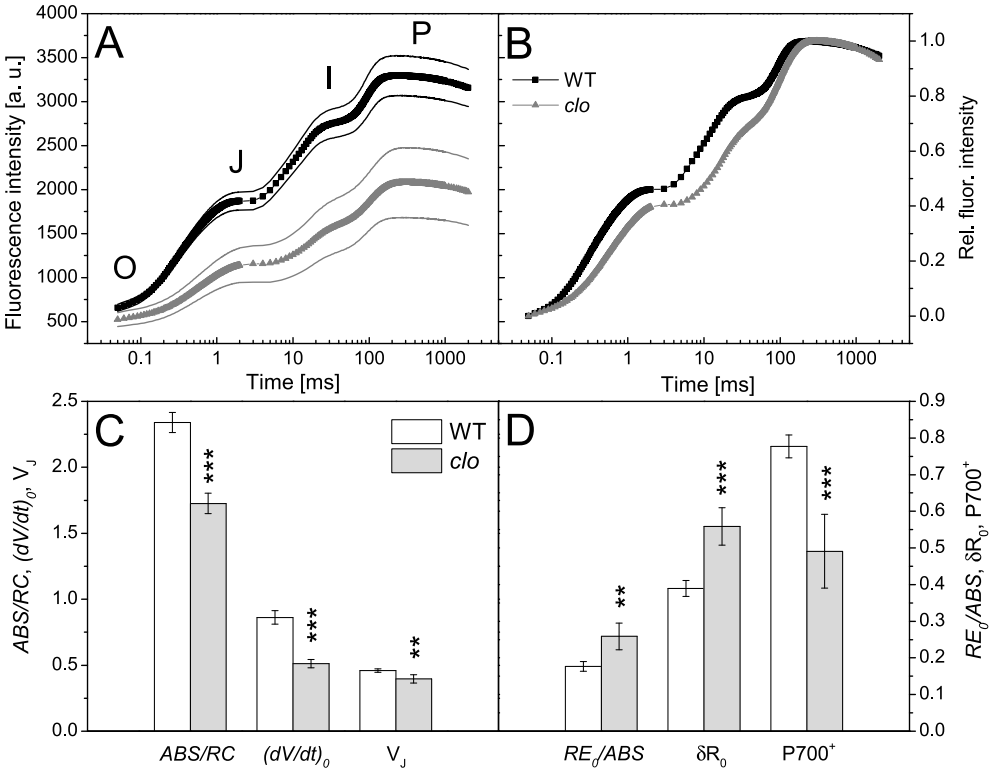


**Fig. 2.** Chl fluorescence induction transient (OJIP curves), related fluorescence parameters and changes in the PSI activity of detached WT and *clo* leaves before senescence induction. A, OJIP curves; B, the normalized OJIP curves; C, the apparent antenna size of active RCII (*ABS/RC*), the initial slope of the O-J fluorescence raise $(dV/dt)_O$, and the relative variable fluorescence at the J-step ($V_J$); D, quantum yield of electron transport from reduced $Q_A$ to final acceptors of photosystem I ($RE_O/ABS$); the efficiency of electron transport from reduced plastoquinone to final acceptors of PSI ($\delta R_0$) and the relative amount of oxidized primary electron donor of PSI, $P700^+$. Means and SD are presented, n = 6–7. Asterisks indicate statistically significant difference (Student's *t*-test) between WT and *clo* (**, P < 0.01; ***, P < 0.001).

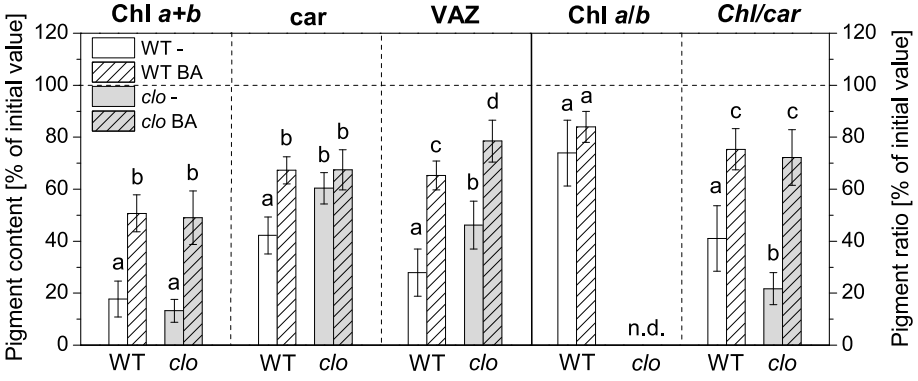


**Fig. 3.** Chlorophyll (Chl *a*+*b*), carotenoid (car) and xanthophyll (VAZ) content related to leaf area and Chl *a*/*b* and *Chl/car* ratios in detached WT and *clo* leaves kept for 4 days in the dark in 0.2% DMSO solution without (−) or with 6-benzylaminopurine (BA). Relative values (% of the initial values before senescence induction) are presented. Means and SD are shown, n = 6. Except of the Chl *a*/*b* ratio (analyzed by the *t*-test, P = 0.139), all other data were analyzed by ANOVA test (P < 0.001 in all cases) and statistically significant differences in following *post hoc* statistical testing (Holm-Sidak test) at P < 0.05 are indicated by different letters.

### 3.3. Effect of BA on senescence-induced changes in WT and clo leaves

To evaluate the effect of cytokinin on dark-senescing WT and *clo* leaves, detached leaves were incubated in BA ($10^{-5}$ mol $l^{-1}$) solution and kept in the dark for 4 days. BA significantly reduced the degradation of photosynthetic pigments in both genotypes, the content of Chl and car decreased by about 50 % and 35 %, respectively (Fig. 3), and the *Chl/car* ratio by about 25 % (Fig. 3). The VAZ content decreased by about 35 % and 20 % in WT and *clo*, respectively (Fig. 3), and the Chl *a*/*b* ratio in WT leaves decreased by about 15 %.

BA also suppressed the senescence-induced decrease in PSII photochemistry in both WT and *clo* leaves (Figs. 4–6). In the presence of BA, $F_v/F_m$ dropped only by 20 % during the senescence, which indicated that PSII photochemistry is relatively well maintained (Fig. 4A). This was also evidenced by a smaller decrease in $\Phi_P$ (i.e., utilization of absorbed light energy by PSII photochemistry) in both WT and *clo* (Fig. 5). In *clo* BA significantly suppressed the senescence-induced increase in $\Phi_{f,D}$ (Fig. 5).

The protective effect of BA on PSII function in senescing leaves was also reflected in less pronounced changes in the shape of OJIP curve (Fig. 6A) and smaller changes in corresponding parameters. In leaves undergoing senescence in the presence of BA, we have observed a smaller increase in relative height of the J-step (i.e., $V_J$) (Fig. 6B) and also the increase in *ABS/RC* and $(dV/dt)_O$ parameters was considerably smaller compared to leaves senescing in the absence of BA (Fig. 6C).

In both genotypes, BA suppressed the senescence-induced decrease in $RE_O/ABS$ and $\delta R_0$; in *clo* the BA application even increased $\delta R_0$ by about 20 % (Fig. 6D). On the contrary, BA had no significant effect on the relative amount of $P700^+$ in either WT or *clo* (Fig. 6D).

The changes in parameters described above indicate that BA suppressed the senescence-induced impairment of PSII photochemistry in both WT and *clo*. Interestingly, in the presence of BA, the progress of senescence in *clo* became more similar to WT (Figs. 4–6), although in the absence of exogenous cytokinin the senescence-induced impairment of PSII function was much more pronounced in *clo*. The stronger effect of BA in the case of *clo* is further apparent from the significantly lower increase in *ABS/RC* and $V_J$ (Fig. 6C). The more marked effect of BA on *clo* in comparison to WT was even more visible when an increased actinic light intensity (600 µmol of photons $m^{-2}$ $s^{-1}$) was applied. In the untreated leaves of WT and *clo*, $\Phi_P$ was 0.13 and 0.14, respectively. In WT, BA improved $\Phi_P$ only non-significantly (to 0.25), while in *clo*, the $\Phi_P$ improvement (to 0.36) was statistically significant.

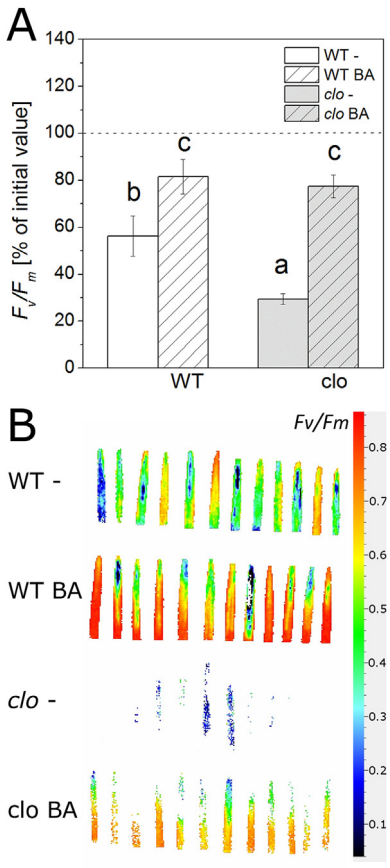


**Fig. 4.** The maximal efficiency of PSII photochemistry in dark-adapted state ($F_v/F_m$) in detached WT and *clo* leaves kept for 4 days in the dark in 0.2% DMSO solution without (−) or with 6-benzylaminopurine (BA). A, the relative $F_v/F_m$ values (% of the initial values before senescence induction), means and SD estimated from measurable leaves are shown. Data were analyzed by ANOVA test ($P < 0.001$) and statistically significant difference in following *post hoc* statistical testing (Holm-Sidak test) at $P < 0.05$ are indicated by different letters. B, $F_v/F_m$ in the area of detached WT and *clo* leaves.

## 4. Discussion

It has been reported that the Chl *b* deficiency accelerates senescence-related changes in rice (Kusaba et al., 2007; Yang et al., 2016). Faster Chl degradation was observed in detached leaves of Chl *b*-deficient rice mutant *cao-2* (Kusaba et al., 2007). Based on faster Chl degradation, increased accumulation of reactive oxygen species, and increased electrolyte leakage Yang et al. (2016) suggested faster senescence in *pgl* rice mutant with reduced Chl *b* content in case of naturally senescing flag leaves as well as in case of detached leaves kept in the dark. Nevertheless, deeper knowledge of senescence-associated impairment of photosynthetic apparatus including PSII and PSI function under Chl *b* deficiency is missing.

To find out whether the deficiency of Chl *b* accelerates senescence-induced impairment of PSII and PSI activities, we have investigated their changes (together with changes in photosynthetic pigment content) in detached leaves of the Chl *b*-deficient barley mutant senescing in the dark for 4 days. As cytokinins are known to partially protect photosynthetic activity during senescence (Oh et al., 2005; Vlčková et al., 2006; Talla et al., 2016), we have also studied the effect of exogenously applied BA and analyzed whether it is able to suppress the senescence-associated changes also in *clo*.

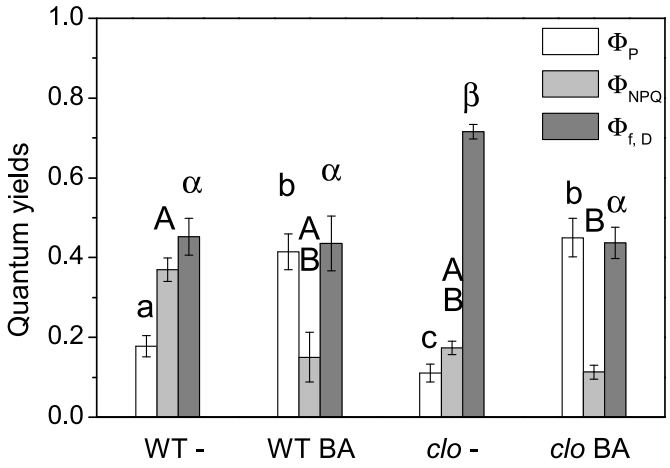


**Fig. 5.** Quantum yields of PSII photochemistry ($\Phi_P$), regulatory non-photochemical quenching ($\Phi_{NPQ}$), and constitutive non-regulatory dissipation processes ($\Phi_{f,D}$) of the detached WT and *clo* leaves kept for 4 days in the dark in 0.2% DMSO solution without (−) or with 6-benzylaminopurine (BA). Means and SD are shown, n = 6. $\Phi_P$ and $\Phi_{f,D}$ were analyzed by ANOVA test ($P < 0.001$ in both cases), followed by *post hoc* statistical testing (Holm-Sidak test) and $\Phi_{NPQ}$ was analyzed by Kruskal-Wallis ANOVA on Ranks test ($P < 0.001$), followed by *post hoc* statistical testing (Dunn's test). Statistically significant differences in the *post hoc* statistical testing at $P < 0.05$ are indicated by different letters.

### 4.1. Lower efficiency of PSII photochemistry in clo mutant before senescence induction

Leaves of *clo* mutant have lower content of photosynthetic pigments (Table 1). As expected due to the mutation in CAO (Mueller et al., 2012) and in agreement with literature (Štroch et al., 2004, 2008), Chl *b* was not detectable in *clo* (Table 1). Due to the lack of Chl *b*, the antenna size of PSII is substantially reduced in *clo*, as has been shown by lower abundance of LHCII proteins (Król et al., 1995; Bossmann et al., 1997) and by changes in emission and excitation Chl fluorescence spectra measured at 77 K (Štroch et al., 2004). We have confirmed the reduced functional size of LHCII in *clo* by lower *ABS/RC* ratio (Fig. 2C), reflecting lower amount of absorbed excitations per active ($Q_A$-reducing) RCII. The presence of smaller PSII antennae resulted in slower supply of excitations to the RCII, in slower $Q_A$ reduction and smaller amount of reduced $Q_A$, which was evidenced by the lower $(dV/dt)_0$ and $V_J$ parameters (Fig. 2C).

Despite the smaller LHCII in *clo*, the efficiency of electron transport behind PSII to PSI was higher compared to WT which corresponds to the higher ratio RCII/RCI in *chlorina f2* mutant reported by Ghirardi et al. (1986). The higher electron flow behind PSII probably led to the lower relative amount of $P700^+$ (Fig. 2D). The reduced size of PSI antennae might also contribute to the decreased relative amount of $P700^+$ as *clo* is known to be deficient in the light-harvesting complex Lhca4 (Bossmann et al., 1997). Consistent with this assumption, it has been shown that kinetics of P700 oxidation was much slower in a rice mutant *dye1-1* with a severely reduced amount of Lhca4 (Yamatani et al., 2018).

The *clo* leaves had slightly less effective PSII photochemistry as indicated by lower values of the maximal quantum yield of PSII photochemistry in the dark-adapted state ($F_v/F_m$; Table 1) and of the maximal and effective quantum yield of PSII photochemistry in the light-adapted state (as $F_v'/F_m'$ and $\Phi_P$; Table 1, Fig. 1D). The slightly lower quantum yield of PSII photochemistry of *chlorina* mutants has been reported previously (Leverenz et al., 1992; Štroch et al., 2004, 2008).

The light energy that is not utilized by PSII photochemistry is dissipated *via* non-regulatory ($\Phi_{f,D}$) and/or regulatory ($\Phi_{NPQ}$) non-photochemical quenching processes. $\Phi_{f,D}$ represents quantum yield of

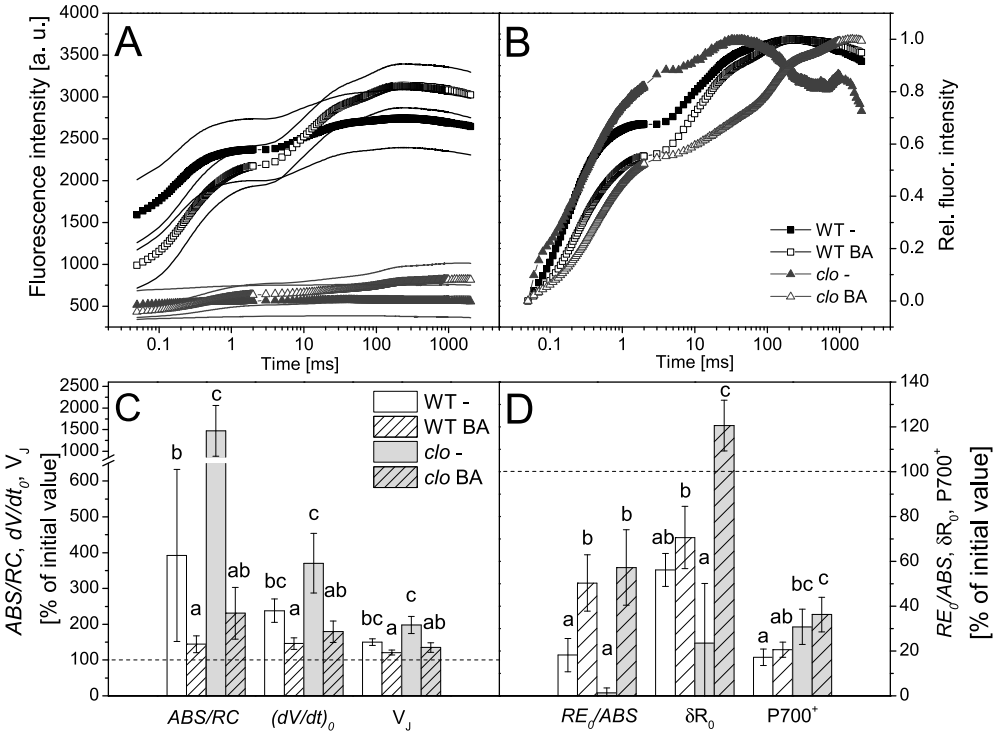


**Fig. 6.** Chl fluorescence induction transient (OJIP curves), related fluorescence parameters and changes in the PSI activity of detached WT and *clo* leaves kept for 4 days in the dark in 0.2% DMSO solution without (−) or with 6-benzylaminopurine (BA). A, OJIP curves; B, the normalized OJIP curves; C, the relative values of the apparent antenna size of active RCII (*ABS/RC*), the initial slope of the O-J fluorescence raise ($dV/dt)_0$, and the relative variable fluorescence at the J-step ($V_J$); D, quantum yield of electron transport from reduced $Q_A$ to final acceptors of PSI ($RE_0/ABS$); the efficiency of electron transport from reduced plastoquinone to final acceptors of PSI ($\delta R_0$) and the relative amount of oxidized primary electron donor of PSI, $P700^+$, expressed as % of the initial values before senescence induction. Means and SD are shown, n = 8–12. Data were analyzed by Kruskal-Wallis ANOVA on Ranks test ($P < 0.001$) and statistically significant differences in following *post hoc* statistical testing (Dunn's test) at $P < 0.05$ are indicated by different letters.

constitutive (basal) energy dissipation (for a review see Lazár, 2015), whereas $\Phi_{NPQ}$ is quantum yield of regulatory quenching, which is induced by illumination to protect the photosynthetic apparatus against excess light and consequent accumulation of reactive oxygen species and oxidative damage (Demmig-Adams et al., 2014). As mentioned above, *clo* had lower $\Phi_P$ (Fig. 1D), which indicates lower utilization of absorbed light energy by PSII photochemistry. The proportion of absorbed light energy allocated into non-photochemical quenching processes was higher compared to WT, as both non-regulatory ($\Phi_{f,D}$) and regulatory component ($\Phi_{NPQ}$) were increased (Fig. 1D).

The regulatory non-photochemical quenching processes are related to activation of the xanthophyll cycle where zeaxanthin (Z) is formed by de-epoxidation of violaxanthin (V) through antheraxanthin (A). The extent of the de-epoxidation is expressed as DEPS. Compared to WT, the *clo* leaves were characterized by higher DEPS, by about 80 % (Table 1). Together with the higher *VAZ/Chl* ratio and higher relative content of car (indicated by the lower *Chl/car* ratio) (Table 1), it implies that the *clo* plants had an enhanced photoprotection of photosynthetic apparatus when they were grown under relatively low light intensity (150 µmol of photons $m^{-2}$ $s^{-1}$). The higher protection against photoinactivation of RCII has been reported by Štroch et al. (2004) in *clo* plants grown under similar light intensity (100 µmol of photons $m^{-2}$ $s^{-1}$). The higher photoprotection of *clo* could be associated with the existence of free (not bound to LHCs) zeaxanthin (Havaux et al., 2007; Štroch et al., 2008; Nezval et al., 2017).

### 4.2. Clo had much more impaired PSII function in dark senescing leaves than WT

It is generally known that leaf senescence is accompanied by the loss of photosynthetic pigments and impairment of photosynthetic function. In the dark senescing leaves, the photochemical activity of PSII is markedly reduced during a few days (Oh et al., 1996; Špundová et al., 2003; Vlčková et al., 2006; Janečková et al., 2018). In the detached leaves of WT, the content of photosynthetic pigments and PSII photochemistry decreased significantly after 4 days in the dark (Figs. 3 and 4). The increase in the *ABS/RC* ratio as well as decrease in the Chl *a/b* ratio indicated that RCII were damaged to a greater extent than LHCII. This is in agreement with higher $(dV/dt)_0$ and $V_J$ parameters (Fig. 6C), indicating increase in the excitation supply into the active RCII, acceleration of $Q_A$ reduction and thus the increased amount of reduced $Q_A$ (Strasser et al., 2000; Stirbet et al., 2018). The PSII photochemistry was impaired as $F_v/F_m$ and $\Phi_P$ decreased (Figs. 4 and 5), whereas the dissipation *via* both regulatory ($\Phi_{NPQ}$) and non-regulatory non-photochemical quenching processes ($\Phi_{f,D}$) increased (Fig. 5). This indicates that the senescing WT leaves were still able to partially regulate the dissipation of excess light energy. The changes in $RE_0/ABS$, $\delta R_0$ and $P700^+$ parameters in the senescing WT leaves indicate that the PSII activity was more impaired during dark senescence than the activity of PSI.

As mentioned above, plants with enhanced Chl *b* content were reported to have slower leaf senescence (Kusaba et al., 2007; Sakuraba et al., 2012), while senescence of Chl *b*-deficient rice mutants was accelerated (Kusaba et al., 2007; Yang et al., 2016). Thus, in the case of *clo* mutant, we expected faster dark-induced senescence. Although the relative decrease in Chl content was similar in WT and *clo* (Fig. 3), the absolute Chl content was pronouncedly lower in the *clo* senescing leaves due to the lower Chl content in the leaves before senescence induction (Table 1). The pronounced decrease in Chl content in *clo* corresponded with more pronounced impairment of PSII function (Figs. 4–6). In fact, the senescing *clo* leaves had only minimal PSII activity after 4 days (Fig. 4B). The preferential senescence-induced impairment of RCII found in the WT leaves was even more pronounced in *clo,* as documented by extremely increased *ABS/RC* (and also by increased $(dV/dt)_0$ and $V_J$, Fig. 6C). Unlike WT, regulatory quenching processes were almost inactive and dissipation *via* non-regulatory processes prevailed, as indicated by pronouncedly increased $\Phi_{f,D}$ (Fig. 5).

Interestingly, despite the more pronounced impairment of PSII photochemistry, the activity of PSI was higher in *clo* than in WT (Fig. 6D). It seems that in the *clo* mutant the missing Lhca4 did not decrease the stability of PSI during senescence.

The substantially impaired PSII function in the dark-senescing leaves of *clo* is in agreement with the previous studies, reporting higher sensitivity of PSII photochemistry of *chlorina* barley mutants to stress-conditions (Leverenz et al., 1992; Peng et al., 2002; Štroch et al., 2008; Tyutereva et al., 2017). This higher sensitivity is probably related to Chl

*b*/LHC deficiency, as proper assembly of LHCII seems to stabilize the structure of PSII complexes and their function (Havaux and Tardy, 1997).

We can summarize that in the *clo* mutant, Chl *b* deficiency caused faster impairment of RCII and consequently faster loss of photochemical activity of PSII during dark senescence. On the contrary, the senescence-induced decrease in PSI activity was smaller in *clo* compared to WT leaves.

### 4.3. Protective effect of exogenous BA on PSII function in dark-senescing leaves was higher in clo

Application of exogenous cytokinins on senescing leaves slows down the degradation of photosynthetic pigments and preserves photosynthetic function, including PSII photochemistry (Oh et al., 2005; Vlčková et al., 2006; Talla et al., 2016; Vylíčilová et al., 2016). In the case of WT leaves, exogenously applied BA significantly reduced the senescence-induced decrease in Chl, car and xanthophyll contents and decrease in the *Chl/car* ratio (Fig. 3), as well as impairment of PSII function (Figs. 4–6). The protective effect of BA was observed also in *clo* and the senescence in the presence of BA was basically similar in both WT and *clo* (Figs. 4–6). Thus, considering the fact that in the absence of BA the PSII function in *clo* leaves was almost completely lost, the protective effect of BA was relatively more pronounced in *clo*. It seems that exogenous BA application suppressed the destabilizing effect of Chl *b*/LHC deficiency on PSII function in the dark-senescing *clo* leaves.

The exact mechanism by which cytokinins maintain PSII function during senescence is not known. It has been proposed that cytokinins could stabilize both LHCII (Oh et al., 2005; Talla et al., 2016; Vylíčilová et al., 2016) and RCII (Oh et al., 2005) in dark-senescing leaves, RCII stabilization being the key process for the maintenance of PSII photochemical activity (Oh et al., 2005). Based on our results we suppose that the protective effect of BA on PSII function in WT as well as in *clo* is based mainly on a pronounced suppression of the impairment of RCII.

## 5. Conclusion

We can conclude that the Chl *b* deficiency in the *clo* barley mutant leads to a substantial acceleration of the inhibition of PSII photochemistry during dark-induced senescence of detached leaves. We assume that this acceleration was due to the more pronounced impairment of RCII. It is in agreement with previous reports, describing higher sensitivity of RCII in *chlorina* mutants to unfavorable conditions (Havaux and Tardy, 1997). The application of exogenous BA was able to suppress the extreme impairment of PSII function in *clo* and the relative extent of the observed protective effect was even more pronounced in *clo* than in WT. It seems that the presence of Chl *b* is not decisive for the protective cytokinin effect on PSII photochemistry in dark-senescing leaves.

Further investigations are needed to clarify the specifics of senescence process in Chl *b*-deficient mutants as well as the mechanism of the cytokinin-mediated protection of photosynthetic apparatus and function in senescing leaves.

## Author contributions

Helena Janečková designed and performed the experiments, analyzed the data, interpreted results and wrote the manuscript; Alexandra Husičková contributed on design and performance of the experiments, helped to interpret the results and revised the manuscript. Dušan Lazár designed the measuring protocol of quenching analysis and measurement of P700 oxidation, evaluated the data, and did statistical analysis; Ursula Ferretti performed the HPLC measurement and analyzed the data; Pavel Pospíšil supervised the HPLC measurement; Martina Špundová supervised the research, contributed on design of the experiments, helped to interpret the results, revised the manuscript and complemented the final writing. All authors read and approved the final manuscript.

## Acknowledgements

This work was supported by Grant No. LO1204 (Sustainable Development of Research in the Centre of the Region Haná) from the National Program of Sustainability I, Ministry of Education, Youth and Sports, Czech Republic, and by ERDF project "Plants as a tool for sustainable global development" (No. CZ.02.1.01/0.0/0.0/16_019/0000827). We thank to Michal Štroch from Department of Physics, University of Ostrava who kindly provided us with seeds of *clo* barley mutants. We also thank to Karel Doležal from Department of Chemical Biology and Genetics (Centre of the Region Haná for Biotechnological and Agricultural Research) who provided us with BA.

## References

Bossmann, B., Knoetzel, J., Jansson, S., 1997. Screening of chlorina mutants of barley (*Hordeum vulgare* L.) with antibodies against light-harvesting proteins of PS I and PS II: absence of specific antenna proteins. Photosynth. Res. 52, 127–136.

Demmig-Adams, B., Garab, G., Adams III., W.W., Govindjee, 2014. Non-photochemical quenching and energy dissipation in plants, algae and cyanobacteria. In: In: Govindjee, Sharkey, T. (Ed.), Advances in Photosynthesis and Respiration, vol. 40 Springer, Dordrecht.

Färber, A., Jahns, P., 1998. The xanthophyll cycle of higher plants: influence of antenna size and membrane organization. Biochim. Biophys. Acta 1363, 47–58.

Gilmore, A.M., Björkman, O., 1994. Adenine nucleotides and the xanthophyll cycle in leaves. I. Effects of $CO_2$- and temperature-limited photosynthesis on adenylate energy charge and violaxanthin de-epoxidation. Planta 192, 526–536.

Ghirardi, M.L., McCauley, S.W., Melis, A., 1986. Photochemical apparatus organization in the thylakoid membrane of *Hordeum vulgare* wild type and chlorophyll *b*-less chlorina f2 mutant. Biochim. Biophys. Acta 851, 331–339.

Havaux, M., Dall'Osto, L., Bassi, R., 2007. Zeaxanthin has enhanced antioxidant capacity with respect to all other xanthophylls in Arabidopsis leaves and functions independent of binding to PSII antennae. Plant Physiol. 145, 1506–1520.

Havaux, M., Tardy, F., 1997. Thermostability and photostability of photosystem II in leaves of the *chlorina-f2* barley mutant deficient in light-harvesting chlorophyll *a*/*b* protein complexes. Plant Physiol. 113, 913–923.

Humplík, J.H., Lazár, D., Fürst, T., Husičková, A., Hýbl, M., Spíchal, L., 2015. Automated integrative high-throughput phenotyping of plant shoots: a case study of the cold tolerance of pea (*Pisum sativum* L.). Plant Methods 11, 20.

Janečková, H., Husičková, A., Ferretti, U., Pržina, M., Pilařová, E., Plačková, L., Pospíšil, P., Doležal, K., Špundová, M., 2018. The interplay between cytokinins and light during senescence in detached Arabidopsis leaves. Plant Cell Environ. 41, 1870–1885.

Krieger-Liszkay, A., Trösch, M., Krupinska, K., 2015. Generation of reactive oxygen species in thylakoids from senescing flag leaves of the barley varieties Lomerit and Carina. Planta 241, 1497–1508.

Król, M., Spangfort, M.D., Huner, N.P.A., Öquist, G., Gustafsson, P., Jansson, S., 1995. Chlorophyll *a*/*b*-binding proteins, pigment conversions, and early light-induced proteins in a chlorophyll *b*-less barley mutant. Plant Physiol. 107, 873–883.

Kusaba, M., Ito, H., Morita, R., Iida, S., Sato, Y., Fujimoto, M., Kawasaki, S., Tanaka, R., Hirochika, H., Nishimura, M., Tanaka, A., 2007. Rice NON-YELLOW COLORING1 is involved in light-harvesting complex II and grana degradation during leaf senescence. Plant Cell 19, 1362–1375.

Lazár, D., 2006. The polyphasic chlorophyll *a* fluorescence rise measured under high intensity of excitation light. Funct. Plant Biol. 33, 9–30.

Lazár, D., 2013. Simulations show that a small part of variable chlorophyll *a* fluorescence originates in photosystem I and contributes to overall fluorescence rise. J. Theor. Biol. 335, 249–264.

Lazár, D., 2015. Parameters of photosynthetic partitioning. J. Plant Physiol. 175, 131–147.

Leong, T.M., Anderson, J.M., 1984. Adaptation of the thylakoid membranes of pea chloroplasts to light intensities. II. Regulation of electron transport capacities, electron carriers, coupling factor (CF1) activity and rates of photosynthesis. Photosynth. Res. 5, 117–128.

Leverenz, J.W., Öquist, G., Wingsle, G., 1992. Photosynthesis and photoinhibition in leaves of chlorophyll *b*-less barley in relation to absorbed light. Physiol. Plantarum 85, 495–502.

Lichtenthaler, H.K., 1987. Chlorophylls and carotenoids: pigments of photosynthetic biomembranes. Methods Enzymol. 148, 350–382.

Mueller, A.H., Dockter, C., Gough, S.P., Lundqvist, U., von Wettstein, D., Hansson, M., 2012. Characterization of mutations in barley *fch2* encoding chlorophyllide *a* oxygenase. Plant Cell Physiol. 53, 1232–1246.

Nath, K., Phee, B.-K., Jeong, S., Lee, S.Y., Tateno, Y., Allakhverdiev, S.I., Lee, C.-H., Nam, H.G., 2013. Age-dependent changes in the functions and compositions of photosynthetic complexes in the thylakoid membranes of *Arabidopsis thaliana*. Photosynth. Res. 117, 547–556.

Nezval, J., Štroch, M., Materová, Z., Špunda, V., Kalina, J., 2017. Phenolic compounds

and carotenoids during acclimation of spring barley and its mutant *Chlorina f2* from high to low irradiance. Biol. Plant. 61, 73–84.
Oh, M.H., Kim, J.H., Zulfugarov, I.S., Moon, Y.-H., Rhew, T.-H., Lee, C.-H., 2005. Effects of benzyladenine and abscisic acid on the disassembly process of photosystems in an *Arabidopsis* delayed-senescence mutant, *ore9*. J. Plant Biol. 48, 170–177.
Oh, S., Lee, S., Chung, I., Lee, C., Nam, H., 1996. A senescence-associated gene *of Arabidopsis thaliana* is distinctively regulated during natural and artificially induced leaf senescence. Plant Mol. Biol. 30, 739–754.
Peng, C., Duan, J., Lin, G., Gilmore, A.M., 2002. Correlation between photoinhibition sensitivity and the rates and relative extents of xanthophyll cycle de-epoxidation in *chlorina* mutants of barley (*Hordeum vulgare* L.). Photosynthetica 40, 503–508.
Sakuraba, Y., Balazadeh, S., Tanaka, R., Mueller-Roeber, B., Tanaka, A., 2012. Overproduction of Chl *b* retards senescence through transcriptional reprogramming in Arabidopsis. Plant Cell Physiol. 53, 505–517.
Špundová, M., Popelková, H., Ilík, P., Skotnica, J., Novotný, R., Nauš, J., 2003. Ultra-structural and functional changes in the chloroplasts of detached barley leaves senescing under dark and light conditions. J. Plant Physiol. 160, 1051–1058.
Špundová, M., Strzałka, K., Nauš, J., 2005. Xanthophyll cycle activity in detached barley leaves senescing under dark and light. Photosynthetica 43, 117–124.
Stirbet, A., Lazár, D., Kromdijk, J., Govindjee, 2018. Chlorophyll *a* fluorescence induction: can just a one-second measurement be used to quantify abiotic stress responses? Photosynthetica 56, 86–104.
Strasser, R.J., Srivastava, A., Tsimilli-Michael, M., 2000. The fluorescence transient as a tool to characterize and screen photosynthetic samples. In: Mohanty, Yunusa, Pathre (Eds.), Probing Photosynthesis: Mechanism, Regulation & Adaptation. Taylor & Francis, London, pp. 443–480.
Štroch, M., Čajánek, M., Kalina, J., Špunda, V., 2004. Regulation of the excitation energy utilization in the photosynthetic apparatus of *chlorina f2* barley mutant grown under different irradiances. J. Photochem. Photobiol. B Biol. 75, 41–50.
Štroch, M., Lenk, S., Navrátil, M., Špunda, V., Buschmann, C., 2008. Epidermal UV-shielding and photosystem II adjustment in wild type and *chlorina f2* mutant of barley during exposure to increased PAR and UV radiation. Environ. Exp. Bot. 64, 271–278.
Talla, S.K., Panigrahy, M., Kappara, S., Nirosha, P., Neelamraju, S., Ramanan, R., 2016. Cytokinin delays dark-induced senescence in rice by maintaining the chlorophyll cycle and photosynthetic complexes. J. Exp. Bot. 67, 1839–1851.
Tyutereva, E.V., Evkaikina, A.I., Ivanova, A.N., Voitsekhovskaja, O.V., 2017. The absence of chlorophyll *b* affects lateral mobility of photosynthetic complexes and lipids in grana membranes of Arabidopsis and barley *chlorina* mutants. Photosynth. Res. 133, 357–370.
Vlčková, A., Špundová, M., Kotabová, E., Novotný, R., Doležal, K., Nauš, J., 2006. Protective cytokinin action switches to damaging during senescence of detached wheat leaves in continuous light. Physiol. Plantarum 126, 257–267.
Voitsekhovskaja, O.V., Tyutereva, E.V., 2015. Chlorophyll *b* in angiosperms: functions in photosynthesis, signaling and ontogenetic regulation. J. Plant Physiol. 189, 51–64.
Vylíčilová, H., Husičková, A., Spíchal, L., Srovnal, J., Doležal, K., Plíhal, O., Plíhalová, L., 2016. C2-substituted aromatic cytokinin sugar conjugates delay the onset of senescence by maintaining the activity of the photosynthetic apparatus. Phytochemistry 122, 22–33.
Yamatani, H., Kohzuma, K., Nakano, M., Takami, T., Kato, Y., Hayashi, Y., Monden, Y., Okumoto, Y., Abe, T., Kumamaru, T., Tanaka, A., Sakamoto, W., Kusaba, M., 2018. Impairment of Lhca4, a subunit of LHCI, causes high accumulation of chlorophyll and the stay-green phenotype in rice. J. Exp. Bot. 69, 1027–1035.
Yang, Y., Xu, J., Huang, L., Leng, Y., Dai, L., Rao, Y., Chen, L., Wang, Y., Tu, Z., Hu, J., Ren, D., Zhang, G., Zhu, L., Guo, L., Qian, Q., Zeng, D., 2016. *PGL*, encoding chlorophyllide *a* oxygenase 1, impacts leaf senescence and indirectly affects grain yield and quality in rice. J. Exp. Bot. 67, 1297–1310.